

Ice Crystallization Induced by Optical Breakdown

B. Lindinger,¹ R. Mettin,¹ R. Chow,² and W. Lauterborn¹

¹*Drittes Physikalisches Institut, Universität Göttingen, Friedrich-Hund-Platz 1, 37077 Göttingen, Germany*

²*Unilever Corporate Research, Colworth Laboratory, Sharnbrook, Bedford MK44 1LQ, United Kingdom*

(Received 8 August 2006; revised manuscript received 29 January 2007; published 25 July 2007)

Ice crystallization in supercooled water has been initiated by focused Nd:YAG laser pulses at 1064 nm wavelength. The pulses of 8 ns duration and up to 2 mJ energy produce a bubble in the supercooled liquid after optical breakdown and plasma formation. The subsequent collapse and disintegration of the bubble into fragments was observed to be followed by ice crystal nucleation in many, but not all cases. Details of the crystallization events have been investigated by high-speed imaging, and nucleation statistics and crystal growth rates are given. It is argued that homogeneous nucleation in the compressed liquid phase is a plausible explanation of the effect.

DOI: [10.1103/PhysRevLett.99.045701](https://doi.org/10.1103/PhysRevLett.99.045701)

PACS numbers: 64.60.Qb, 42.62.-b, 47.55.dp, 81.10.-h

Introduction.—Nucleation of the solid phase in a supercooled liquid can be initiated by different mechanisms [1]. It can be distinguished between homogeneous nucleation, where statistical density and structure fluctuations in the pure bulk liquid cause an embryo crystal to grow, and inhomogeneous nucleation, where the presence of a boundary, a particle, or another type of contamination facilitates this process. Furthermore, several variations of dynamic stimulations of nucleation are known [2]. Among them, ultrasonic vibration (“sonocrystallization”) has been reported [3]. It has been shown before that sonocrystallization of supercooled liquid is mediated by cavitation, and, in particular, by bubble collapse [4]. The process of nucleation has even been initiated experimentally by a single acoustically levitated cavitation bubble [5,6]. Although the detailed mechanism is not proven yet, a good candidate for the nucleation trigger is the strong compression in a pressure wave close to the collapsing bubble [7–10].

In this Letter, we show that an optical breakdown, followed by a cavitation bubble and its collapse, is able to trigger solidification of supercooled liquid water. By high-speed imaging we investigate the nucleation process on small temporal and spatial scales, and nucleation statistics and crystal growth dynamics are reported. We estimate the conditions in the liquid close to the collapsed bubble and show that the observations are consistent with homogeneous nucleation in the emitted pressure wave.

Experimental setup.—The experimental setup is shown in Fig. 1. Demineralized and filtered (20 μm pores) water in a rectangular glass cuvette ($25 \times 25 \times 65 \text{ mm}^3$) was cooled. The water temperature was constantly monitored by a thermocouple submerged from the top, and which was never observed to be a nucleation point. The glass cuvette was contained within a larger rectangular transparent cooling bath cell (PMMA). The cooling liquid (ethylene glycol/water 50/50 by volume) was kept at a controlled temperature by a staged cooler with Peltier device. The outer cell was held within a nitrogen atmosphere to isolate the walls against air humidity. While water in very small samples or

confined geometry can be supercooled down to less than -40°C [11], our cuvette could reach a minimum of $-8.3 \pm 0.5^\circ\text{C}$ before spontaneous nucleation occurred (probably from the walls). From one side, a Nd:YAG pulsed laser (Lumonics HY 750, wavelength 1064 nm, pulse length 8 ns) was coupled into the setup via a focusing lens ($f = 30 \text{ mm}$, focusing angle 19°). The lens was mounted outside the cooling liquid cell, and the focal spot of the laser was centered in the inner cuvette. Events were recorded from the side by a high-speed CCD camera (KSV HiSIS 2002, 1120 frames per second, 800 μs exposure time, 256×256 pixels, 8 bit) with background illumination. The laser energy was adjusted by gray filters to be slightly above the threshold to achieve breakdown, which is around 1 mJ in distilled water for the pulse length and focusing angle used [12,13]. The statistical process of plasma formation in the filtered water resulted in a significant amount of laser shots without optical breakdown and therefore without cavitation bubble. None of these shots ever produced ice.

High-speed recordings.—Two examples of optical breakdown with subsequent ice nucleation are shown in Fig. 2 for different water temperatures (-7.25°C and -4.20°C). Just at the end of the exposure of frame 0, the laser shot was initiated, and the plasma is visible as a bright region in the center. The dynamics of the subsequently

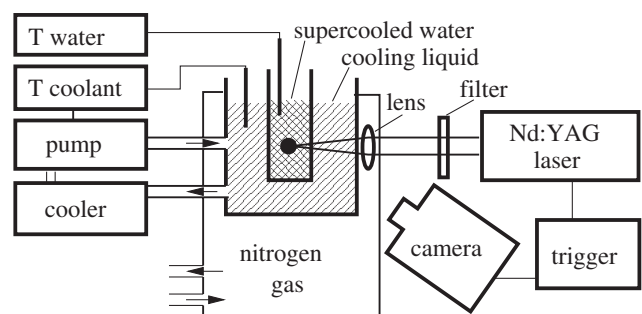


FIG. 1. Schematic setup of experiment (not to scale).

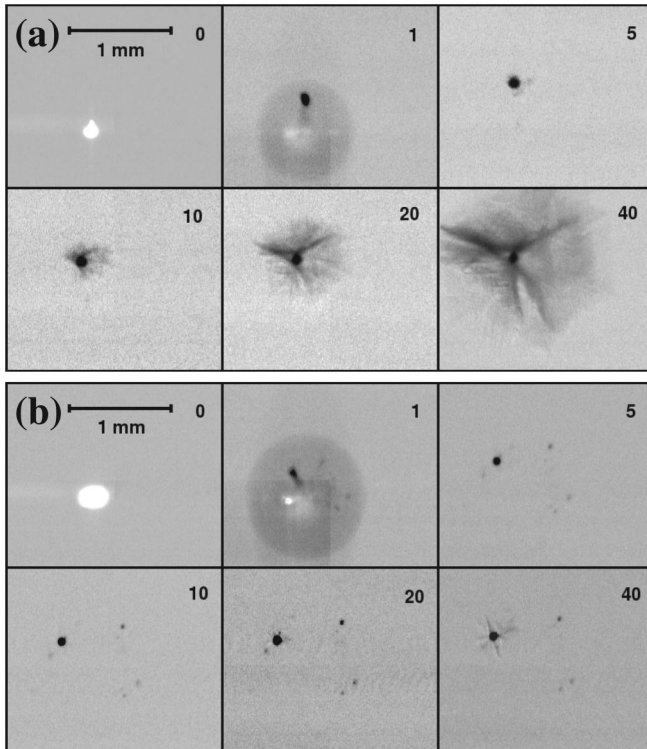


FIG. 2. Ice crystallization induced by optical breakdown and subsequent bubble dynamics. Selected frames from two high-speed recordings; interframe time $888 \mu\text{s}$, frame numbers and size given in the figure. (a) $T = -7.25^\circ\text{C}$, $R_{\text{max}} = 474 \pm 2 \mu\text{m}$; (b) $T = -4.20^\circ\text{C}$, $R_{\text{max}} = 584 \pm 2 \mu\text{m}$.

forming bubble, i.e., its sudden growth and collapse, takes place within about $100 \mu\text{s}$ [14], which is completely within the exposure time of frame 1. The bubble's maximum extension can be identified on this frame as a dark gray shadow, and the maximum radius R_{max} can be measured. After collapse, remnant bubbles remain: one bigger fragment in (a) and several fragments in (b). They contain noncondensable gases, probably mainly H_2 and O_2 and traces of further reaction products of water and air [15]. Typically, remnant bubbles or bubble fragments are observed to move away from the plasma center position, apparently driven by momentum from an aspherical collapse of the laser bubble. In Figs. 2(a) and 2(b), this motion is directed upwards and left upwards, respectively. Without ice nucleation taking place, the remnants finally disappear by rising up and dissolving. In the shown examples, however, ice crystallizes, and it forms directly next to a remaining bubble. For the lower temperature in Fig. 2(a), this can readily be detected in frame 5, i.e., about 4 ms after the laser shot. Frames 10, 20, and 40 in Fig. 2(a) show the further growth of the crystal at this nucleation site, which remains the only one in the whole sample. At higher temperature, the nucleation can optically be identified only later. In Fig. 2(b), the first clear indications of a crystal appear around frame 10 (after about 9 ms). In this case, at

least five fragments have been formed in the bubble collapse, but like in (a), ice is growing only at one site (the largest bubble fragment). Nucleation at more than one point has also been observed in some cases (not shown here), and then crystals grew usually next to visible remnant gas bubbles.

Nucleation statistics.—The laser pulse energy showed a certain jitter (≈ 1 to 2 mJ), and accordingly we observed variations in maximum bubble size and bubble shape. High asphericity and visible jetting during collapse is often preceded by higher laser shot energy, elongated plasma extension and larger maximum bubble radius. It leads to more bubble fragments, which also move faster. Less energetic optical breakdowns, resulting in more spherical plasmas and smaller maximum radii, gave less fragments, and frequently ended in just one visible remnant, like in Fig. 2(a). We tried to correlate laser energy, maximum bubble radius, and bubble fragmentation to the occurrence of ice nucleation events. However, there was no significant correlation, which is the reason why we omit these data. The only discernible correlation was between temperature and nucleation: the larger the supercooling, the more likely are laser bubble induced crystallization events. This is shown in Fig. 3. There is a supercooling threshold at -2°C above which no ice nucleation by optical breakdown could be initiated. Furthermore, the probability of crystallization seems not to approach unity if the supercooling reaches the level of spontaneous nucleation occurring without any stimulus.

Nucleation timing and crystal growth rate.—The high-speed recordings have been used to analyze the crystal size evolution in time. In the case of a nucleation, the solid phase became visible some milliseconds after the laser plasma. The detectable size was limited by optical resolution and low contrast of the ice to about $30 \mu\text{m}$. The crystals are expected to grow linearly in time with the growth rate being higher at lower water temperature [16]. This has been confirmed, as is shown in Fig. 4 for some selected nucleation events. It is interesting to observe that

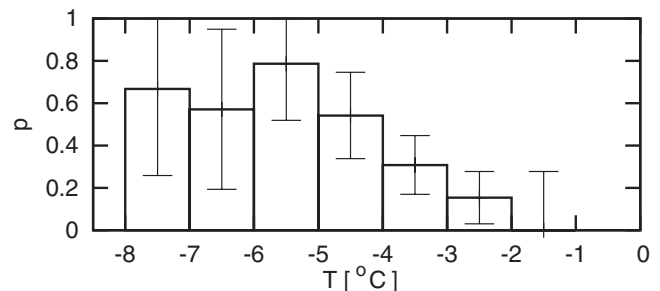


FIG. 3. Relative frequency p of laser bubble initiated nucleation events vs water temperature T . Data given for temperature intervals of full degrees centigrade; error bars indicate $\pm 1/\sqrt{N}$ intervals, where N is the number of total shots with optical breakdown (nucleating and non-nucleating) within the indicated temperature interval.

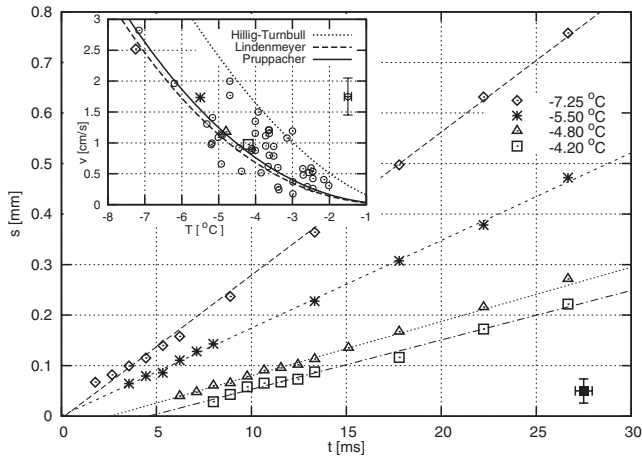


FIG. 4. Ice crystal radius s vs time t after laser shot: four examples for different supercoolings (values given). Symbols: measurements, lines: linear fits. Uncertainties given by error bars in the bottom right and correspond to single frame exposure time and ± 3 pixels. Inset: Rate of ice growth v vs bulk temperature T . Symbols as in main figure indicate the respective data; circles are other nucleation events. Lines indicate empirical relations. Uncertainties estimated and given by error bars at the right of the inset.

for small supercooling, the growth of laser bubble induced crystals appears to be delayed relative to the laser shot (or bubble collapse): the backwards extrapolated linear fit crosses the time axis significantly off zero. This will be discussed later.

Growth rates of laser induced crystals are given vs the water temperature T in the inset of Fig. 4. Here the rate v is defined as the time derivative (after a linear fit) of the measured distance of the fastest growing ice front (dendrite tip) to the origin next to a remnant bubble. Because of the projection into the camera plane this is a lower bound of the true ice front velocity, which might be larger. Empirical relations in the form of $v = a|T|^\kappa$ [cm/s] are drawn as well in the inset. They are according to Hillig and Turnbull ($a = 0.158$, $\kappa = 1.69$ [16]), Lindenmeyer *et al.* ($a = 0.028$, $\kappa = 2.3$ [7,17]), and Pruppacher ($a = 0.035$, $\kappa = 2.22$ [18]). Our data show relatively large scatter, but fall closer to the latter two curves which have been obtained by free crystal growth far from a solid surface. This is consistent with the fact that the laser nucleated ice crystal fronts propagate almost ideally in the free liquid.

Preexisting bubbles.—If laser pulses were applied repetitively, it happened that remnant bubbles from a previous, nonfreezing laser plasma have been present in the supercooled liquid close to the newly generated laser bubble. Interestingly, in almost all such cases observed, freezing took place next to a preexisting bubble. One example is shown in Fig. 5. The collapse dynamics of the laser induced bubble is very aspherical and creates many bubble fragments due to jetting. The maximum bubble size and the strongly distorted bubble shape can be seen as gray silhou-

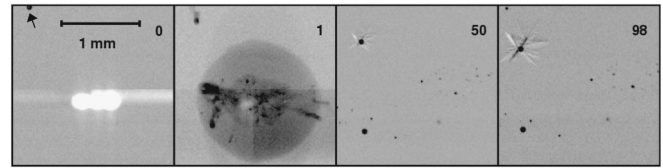


FIG. 5. Laser induced ice nucleation at preexisting bubble (arrow). Frame numbers and scale given in the figure; $T = -2.71$ °C, $R_{\max} = 768 \pm 2$ μ m.

ettes on frame 1. An old remnant bubble of 36 ± 2 μ m radius is visible at the top left (arrow in frame 0), and it is accelerated downwards by the collapse flow field. Crystal growth initiates in this case *only* at this preexisting bubble, as can be seen on the following frames. In other experiments, ice nucleation at both preexisting *and* new remnant bubbles has also been recorded. However, it appeared that at preexisting bubbles ice was nucleated *always* if they were sufficiently close to the laser focus, i.e., in the range of about 2 mm.

Discussion.—The ice nucleation by optical breakdown and subsequent bubble dynamics is strongly related to sonocrystallization, where acoustic cavitation bubbles cause freezing [2,3]. The physical effects of a laser bubble collapse (luminescence, surface erosion) are very similar to the collapse effects of cavitation bubbles created by an acoustic field [14]. In particular, both optically and acoustically generated bubbles can emit strong pressure waves, which could trigger the actual crystal nucleation [7–10]. Additional to the bubble collapse pressure wave, in our setup a first, alike pressure wave is created by the optical breakdown itself, which converts roughly 50% of the laser pulse energy into sound [13]. For a similar experimental setup both pressure fronts have been measured and extrapolated to lie well above 10 kbar close to the plasma and the collapsed bubble, respectively [19]. From the adiabatic compression lines given by Hickling ([10], Fig. 3) we conclude that shock pressures above 10 kbar cause substantial additional supercooling. For 30 kbar, an effective supercooling of -40 K can be read off. Akhatov *et al.* [20] have calculated in a numerical study pressures and temperatures in collapsing laser induced bubbles under conditions almost identical to our experiments. They provide also data for the liquid close to the collapsing bubble. From their Figs. 7 and 8 we conclude that (i) the volume V_p of liquid that is exposed to pressures of 30 kbar and above can be estimated by a spherical shell of 5 μ m thickness around the bubble core of 20 μ m radius, (ii) the duration of compression to 30 kbar and above can be estimated to an amount $\Delta t \approx 5$ ns, which should be sufficiently long to form ice nuclei [5], and (iii) heat conduction from the compressed hot bubble core is too slow to increase significantly the temperature of the considered liquid shell within 5 ns. Thus, for the observed nucleation of order one ice crystallite per bubble collapse (laser shot), a nucleation rate

of $J = 1/(V_P \Delta t) = 6.3 \times 10^{15} \text{ cm}^{-3} \text{ s}^{-1}$ is needed. Unfortunately, no experimental data for homogeneous nucleation rates of water at the estimated conditions of high pressures are known to the authors. Therefore, we take as rough values for comparison the nucleation rates at a supercooling of -40 K for normal pressure, as reported in [11,21]. These values fall into the range of 10^{12} to $10^{15} \text{ cm}^{-3} \text{ s}^{-1}$. In view of the given uncertainties, we take this agreement in order of magnitude as an indication that homogeneous nucleation in the compressed liquid phase is a plausible mechanism for the observed nucleation [22]. A similar estimate holds for homogeneous nucleation in the primary pressure wave launched by the laser plasma.

To explain retarded crystal growth for weaker supercooling and prevented nucleation above $-2 \text{ }^\circ\text{C}$, the local energy deposition by the laser shot might be responsible. Part of the laser energy is lost by acoustic radiation and chemical reactions, but roughly half of it is finally converted into local heating of the liquid [13]. This would be enough to raise the temperature of a liquid shell of a few hundred μm around the remnant bubbles uniformly by 2° . Because heat conduction is slower than the pressure wave, it might even be possible that a once nucleated crystal is run over by the warming front shortly later, and melts again. In such a case a macroscopic crystal would not be observed (see also [10] for discussion of a “temporal ice nucleation”). If a macroscopic crystal grows, its growth rate at some distance from the nucleation point is finally determined by the bulk temperature (Fig. 4). The local heating could also explain the preferred nucleation at preexisting neighboring bubbles. They collapse violently after being hit by the primary shock, causing positive pressures of probably the same order of magnitude as the breakdown induced wave or the laser bubble collapse wave [25], however, in a non-heated zone of the liquid.

Conclusion.—It was shown that ice nucleation in supercooled water can be triggered by the optical breakdown induced by a focused Nd:YAG laser pulse. The proposed mechanism behind this effect is homogeneous nucleation in the strongly compressed liquid: One first pressure wave is generated by the breakdown plasma expansion, and one or more secondary pressure waves are created at collapse of the laser produced bubble or neighboring bubbles. Quantitative estimates of pressures and affected liquid volumes support this mechanism. The observed probability of ice crystallization caused by the breakdown is zero above $-2 \text{ }^\circ\text{C}$, grows with larger supercooling, but does not reach unity. At lower supercooling, crystal growth can appear retarded. These observations can be explained qualitatively by heat conduction from the hot plasma spot impeding crystal growth. Measured growth rates (after the initial phase) scatter within regions reported in the literature. Possible applications of the effect include a tempo-

rally and spatially selective nucleation of supercooled transparent liquids.

The authors thank T. Kurz, R. Geisler, B. Wolfrum, and the workshops of the Drittes Physikalisches Institut for help and discussions.

-
- [1] B. Chalmers, *Principles of Solidification* (J. Wiley & Sons, New York, 1964).
 - [2] B. Chalmers, in *Liquids: Structures, Properties, Solid Interactions*, edited by T.J. Hughel (Elsevier, New York, 1965), p. 308.
 - [3] R. W. Wood and A.L. Loomis, *Phil. Mag.* (VII) **4**, 417 (1927); S. Hem, *Ultrasonics* **5**, 202 (1967); T.C. Bhadra, *Indian J. Physics* **42**, 91 (1968); S.N. Gitlin and S. Lin, *J. Appl. Phys.* **40**, 4761 (1969); T. Inada *et al.*, *Int. J. Heat Mass Transfer* **44**, 4523 (2001); **44**, 4533 (2001); R. Chow *et al.*, *Ultrasonics* **43**, 227 (2005); R. Chow-McGarva, Ph.D. thesis, University of Leeds (UK), 2005.
 - [4] J.D. Hunt and K.A. Jackson, *J. Appl. Phys.* **37**, 254 (1966).
 - [5] K. Ohsaka and E.H. Trinh, *Appl. Phys. Lett.* **73**, 129 (1998).
 - [6] R. Chow *et al.*, *Proceedings of the IEEE Int. Ultrasonics Symposium, Honolulu, Hawaii, 2003* (IEEE, Piscataway, 2003), p. 1447.
 - [7] R. Hickling, *Nature (London)* **206**, 915 (1965).
 - [8] M.N. Plooster, *Nature (London)* **217**, 1246 (1968).
 - [9] C.P. Lee and T.G. Wang, *J. Appl. Phys.* **71**, 5721 (1992).
 - [10] R. Hickling, *Phys. Rev. Lett.* **73**, 2853 (1994).
 - [11] H.R. Pruppacher and J.D. Klett, *Microphysics of Clouds and Precipitation* (Kluwer, Dordrecht, 1997).
 - [12] F. Docchio *et al.*, *Appl. Opt.* **27**, 3661 (1988).
 - [13] A. Vogel *et al.*, *Appl. Phys. B* **68**, 271 (1999).
 - [14] W. Lauterborn and H. Bolle, *J. Fluid Mech.* **72**, 391 (1975).
 - [15] G. Maatz *et al.*, *J. Opt. A Pure Appl. Opt.* **2**, 59 (2000).
 - [16] W.B. Hillig and D. Turnbull, *J. Chem. Phys.* **24**, 914 (1956).
 - [17] C.S. Lindenmeyer *et al.*, *J. Chem. Phys.* **27**, 822 (1957).
 - [18] H.R. Pruppacher, *J. Chem. Phys.* **47**, 1807 (1967).
 - [19] O. Lindau, *Untersuchungen zur lasererzeugten Kavitation* (Der Andere Verlag, Osnabrück, Germany, 2001).
 - [20] I. Akhatov *et al.*, *Phys. Fluids* **13**, 2805 (2001).
 - [21] C.A. Jeffery and P.H. Austin, *J. Geophys. Res.* **102**, 25 269 (1997).
 - [22] For a theoretical estimation of the nucleation rate in the pressure wave, it is interesting to note that the standard theory of nucleation [23,24] predicts for water at 30 kbar a nucleation activation energy barrier of the order of kT , which appears consistent with homogeneous nucleation. The more elaborated theory [21] does unfortunately not reach the very high pressure region.
 - [23] L. Landau and I.M. Lifschitz, *Lehrbuch der Theoretischen Physik* (Akademie-Verlag, Berlin, 1987), Vol. V, Chap. 162.
 - [24] S. Balibar and F. Caupin, *C.R. Physique* **7**, 988 (2006).
 - [25] O. Lindau (unpublished).